Relaxing conjugacy to fit modeling in dynamical systems

Joseph D. Skufca* and Erik M. Bollt†
Department of Mathematics, Clarkson University, Potsdam, New York 13699, USA
(Received 26 January 2007; revised manuscript received 21 June 2007; published 31 August 2007)

We address a fundamental modeling issue in science as related to the field of dynamical systems: when is a model of a physical system a ÒgoodÓ representation? Conjugacy provides a means to determine if two systems are dynamically equivalent. We develop mathematical technology to decide when dynamics of a ÒtoyÓ model are like (although not identical to) dynamics of the physical system, since the concept of conjugacy is too rigid for such cases. We contrast the usual methodology where model quality is measured in a Banach space to our dynamically motivated notion of matching orbits as best as possible. We highlight our methods with a lower-ordered model of a "noisy" logistic map and also a simplified model of a Lorenz system such that the usual one-dimensional map model is not exactly justified in the traditional sense.

DOI: 10.1103/PhysRevE.76.026220 PACS number(s): 05.45.Gg, 05.45.Pq, 82.20.Wt, 87.15.Aa

I. INTRODUCTION

A standard approach to quantifying model accuracy is to measure how "close" the model is to the original system. Often overlooked, however, is that defining "close" depends upon what aspects of the system we are trying to model. In many cases, *prediction* is our modeling goal, such as when forecasting the weather. The quality of prediction is grounded in numerical analysis on Banach spaces: the "goodness" of short term predictions is based on measurement of residual error. However, in *dynamical systems*, a model's quality is typically *not* based on such error analysis. Continuing, for sake of example, in the field of meteorology, we cite a famous historical example to highlight this long recognized issue. Consider Lorenz's 1965 paper about his 28-variable ordinary differential equation model of the weather [1] which consists of a Galerkin's projection of a two-level geostrophic model of atmospheric fluid flow. About the matter of choice of parameter values which are initially free in the model, the tuning of which leads to dramatically different dynamic behavior due to a plethora of possible bifurcations, Lorenz says: "Our first choice of constants lead to periodic variations. Subsequent choices yielded irregular…." Expert knowledge as a meteorologist concerning what "reminded" him of realistic weather oscillations guided the model choice. He used a similar modeling approach even by the time of his 1998 paper on a 40-variable model [2]. As modeling moves across the sciences, the applied dynamical systems community still tends to choose the "best model" from a model class in an intuitive manner.

In general, when one proposes a mathematical model for some system, the model provides a simplified representation. Modeling can be viewed as the art and science of choosing a "good" representation, where the evaluation of the model's "goodness" is based on how well it satisfies the *purpose* for which we are modeling. For example, if we want a simplified representation of the relationship between two variables in a system such that given one, we could predict the other, techniques of approximation theory can find a mathematical model that matches data collected from the system. Choosing an appropriate description of "error" in the problem (least squares, square integral, maximum, etc.) we can find a well-defined "best" model for our system within a model class (linear functions, for example). The field of dynamical systems provides an alternative purpose to the modeling process, focusing not on predicting behavior of the system, but rather, on qualitative characterization of the system. The three-variable Lorenz system illuminates the richness of behavior that might be created by a convection flow, but is not meant for actually computing that flow. Since the beginnings of the field of dynamical systems by Henri Poincaré [3], characterizing a dynamical system asked us to examine topological and geometric features of orbits, rather than focusing on the empirical details of the solution of the dynamical system with respect to a specific coordinate system. One seeks to understand coordinate independent properties, such as the periodic orbit structure—the count and stability of periodic orbits. The question of whether two systems are dynamically the same has evolved into the modern notion of deciding if there is a conjugacy between them [4–8].

Given these notions, we often speak of a "toy model"—a dynamical system which is much "like" the "real" system. These subjective evaluations are assertions that the model is *satisfactory,* but fails to distinguish excellent models from fair ones. We assert that *quantifying the quality* of a model is an essential problem in science. A primary interest of this work will be to develop principles and methods to compare dynamical systems when they are *not* necessarily equivalent (in the sense of conjugacy), but in a manner which respects conjugacy.

II. BACKGROUND

Given two dynamical systems, $g_1: X \to X$, and $g_2: Y \to Y$, the fundamental departure from a typical measurement of approximation between the two dynamical systems is that we do not directly compare g_1 and g_2 under an embedding in a Banach space (e.g., measuring say $\|g_1 - g_2\|_{L^2}$) because such measurements pay no regard to the central equivalence relationship in dynamical systems—conjugacy. Two systems are

*jskufca@clarkson.edu
†ebollt@clarkson.edu

conjugate if there is a homeomorphism $h:X\to Y$ between the underlying phase space (h must be 1-1, onto, and continuous and h^{-1} must be continuous), and h must commute the mappings at each point $x\in X$, such that $h\circ g_1=g_2\circ h$. Practically, h represents an "exact" change of coordinates so that the mappings behave exactly the same in either coordinate system. We give the name "commuter" to any function $f:X\to Y$ satisfying the commuting relationship

$$f\circ g_1 = g_2\circ f, \tag{1}$$

and note that a commuter will be a conjugacy only if it is a homeomorphism. The commuter provides a matching between trajectories for g_1 and g_2; over and/or underrepresentations are reflected as 1-1 and onto problems in f, while trajectories that permit matching only for finite time are related to discontinuities in f. We develop measures of commuters f that quantify "how much" the f may fail to be a homeomorphism, which we call *homeomorphic defect.* Our fundamental contribution is that we note that measurement of *defect* allows us to quantify the dissimilarity of g_1 and g_2 in a manner that is consistent with the dynamical systems approach. We remark on the broad applicability of our approach: if a mathematical model is a *simplified* description of some system, then the model obviously is not *equivalent* to the system; therefore the two are *not* conjugate. Our research addresses this issue of *quantifying the quality* in a mathematically grounded manner.

III. PROTOTYPICAL EXAMPLE: MODELING A NOISY LOGISTIC MAP

It is well-known that the logistic map $g_1(x)=rx(1-x)$ is conjugate to the tent map $g_2(x)=a\left(1-2\left|x-\frac{1}{2}\right|\right)$ for parameter values $r=4$ and $a=2$. The conjugacy $h(x)=\frac{1}{2}[1-\cos(\pi x)]$ provides perhaps the most studied example in the pedagogy of dynamical systems for teaching conjugacy. However, if r is perturbed even slightly, the conjugacy is broken. Now consider a system with a much stronger perturbation, like a noisy version of the logistic map of Fig. 1(a) using parameter value of $r=3.83$ for the "prenoise" system. The noised version is obviously not conjugate to a simple tent map. The commuter shown in Fig. 1(b) is not a homeomorphism, since it fails at least one-one-ness, which we see immediately by direct inspection. The commuter gives an orbit equivalence between the two maps and is the key to understanding the quality of a model. One could argue that the tent map shown is a good candidate to model this "noisy logistic map"—it simplifies the small scale dynamics while capturing the primary dynamics of the large scale orbit structure.

On the other hand, a common pragmatic approach is to smooth data, perhaps by a best least-squares model within a model class such as $\hat{g}_2(x)=a_2x^2+a_1x+a_0$. Alternatively, one might choose to smooth the data, perhaps by using a smoothing spline method [20] where the modeler must choose a value for a given smoothing parameter [9–11]. This approach is common in experimental science, and we have used it ourselves, as in our own work for modeling the symbolic dynamics of the Belousov-Zhabotinsky reaction chemical

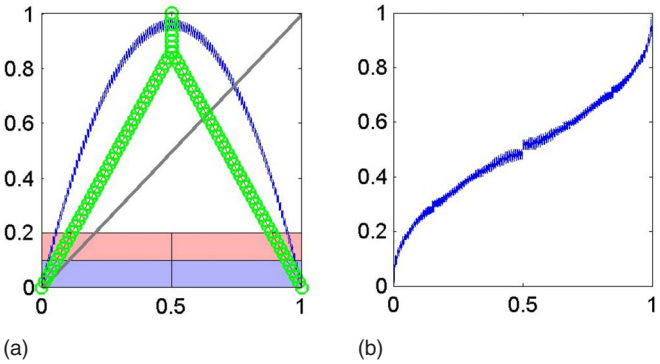

FIG. 1. (Color online) Modeling a noisy logistic map. (a) Map g_1, nearby the logistic map $3.83x(1-x)$ in any $L^p([0,1])$, $p\geq 1$ [but not in the $C^1([0,1])$ norm], was constructed by perturbing the logistic map to force slope $|g_1'(x)|=10$ everywhere that it exists. The stable period-three orbit is destroyed by the noise. The circles graph a tent map g_2 (with vertical extension) which is our "best" model within the family of symmetric tent maps. (b) The resulting commuter f between g_1 and this tent map g_2 is reminiscent of the homeomorphism $h(x)=\frac{1}{2}[1-\cos(\pi x)]$ between the full logistic map and the full tent map. However, whereas h is a diffeomorphism, f is not even a homeomorphism, though the visual impression is that we would not need to move the points (on the graph of f) very far to achieve a homeomorphism.

system known only through measured data [12,13] as depicted in Fig. 2. Invariably, noise and errors corrupt the signal, and it is appropriate to simplify the data—standard practice in science. Our point is that *modeling choices* must be made, whether it is how strong to tune the smoothing parameters μ in the smoothing spline, what model class (quadratic, cubic, etc.), or how to handle boundary conditions. Such choices yield slightly different models, none of which are likely to be conjugate to each other, nor to whatever might be the "true" dynamics. In each of these pragmatic approaches, the judgment of quality for the minimization step is in a Banach space, usually within the L_2 norm, which is completely blind to the concept of conjugacy and dynamics. Consequently, there is no *a priori* reason to expect this modeling approach to be successful if the modeler's intent is to capture the *topological dynamics*, because it selects a model that optimizes the wrong thing. (Although we note that we have employed this approach ourselves in [12,13].)

Defect measure of a commuter is designed to compare model to data within the context of dynamical systems rather than prediction. For example, the blue data set in Fig. 1 could be simply modeled by a smoothing spline, and that approach has an appropriate context, such as minimizing the short term prediction error between model and the system. However, if the modeler wants to ignore the "noise" but describe the underlying dynamics, then this simple approach leads to some difficulties: An optimal denoising (in an L_2 sense) should return the underlying map $g(x)=3.83x(1-x)$, which lies in the "period-three window." The smoothed map would have a stable period-three orbit as its attractor, whereas the original dynamics are transitive on an interval, and the defect is large. The choice to model using *tent maps* provides a model class that is simple, well-understood, easy

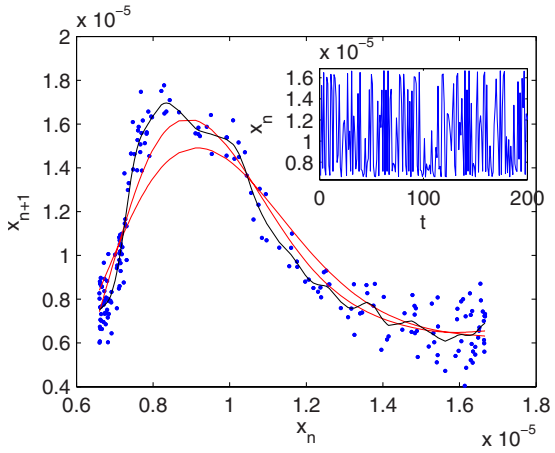

FIG. 2. (Color online) On smoothing and modeling. A common practice when confronted with real world data is to apply a popular smoothing filter, such as fitting a least-squares model from a model class, or a smoothing spline such as shown here for a return mapping of a data set of reactant concentrations from a Belousov-Zhabotinsky reaction [12,13], with time-series inset. Different choices of model parameters yield different "fitted" models all with differing dynamical characteristics. The smoothing process does not optimize with respect to dynamics, but, rather, with respect to an assumed normed linear space. From the very relaxed curvature (the shorter peaked red curve) to the middle curvature model (the higher red curve), we observe models that could be represented by a subshift on two symbols (though the shifts are not topologically equivalent). For the (tallest) black curve, with the largest allowed curvature of the three curves, we create dynamics of a many symbol shift space. The choice of the curvature parameter which is "best" for some application is typical of the type of decision that confronts a modeler who must often rely on "expert knowledge" to select the model.

to analyze, and which should be sufficient to describe the "larger" dynamics while ignoring the "noise;" but if the modeler were to select a tent map that minimizes the L_2 error, it will *not* provide the best description of the topological dynamics. We suggest that choosing the tent map that minimizes the defect of the commuter function is truer to the notion of dynamical systems. As to the choice of the family of tent maps to choose our model, we continue the argument: In many contexts, we are more interested in modeling the topological dynamics than we are with prediction. Certainly there are smooth one-humped maps of all varieties which could be fitted to those data sets in either of Figs. 1 and 2, and generally, the result will suitably describe the dynamics. However, it is often important to have a dynamically "simple to analyze" model instead. Such has been the role of the tent maps, mod-shift maps, and Renyi' maps in general. For this reason, throughout this work, we have generally chosen piecewise linear maps with balanced slopes, as we believe it is a standard modeling class to be employed when *topological* dynamics are of primary concern.

IV. MEASURING DEFECT DEVIATION FROM CONJUGACY

We have argued above that inspection of the commuter function f between two dynamical systems $g_1: X \to X$ and $g_2: Y \to Y$ is a natural way to understand the similarity of two dynamical systems, which we roughly call "mostly conjugacy." We will use measure-theoretic tools to quantify appropriate characteristics of f. Our introduction of mostly conjugacy is a measure theoretic construction related to the topological notion of almost conjugacy and orbit equivalence found in the symbolic dynamics literature [5,14]. We assume $f: D \to R$ satisfies the commutative relationship (1). In [15], we define a *homeomorphic defect of* f, denoted $\lambda(f)$, as a convex combination

$$\lambda(f) = \alpha_1 \lambda_O(f) + \alpha_2 \lambda_{1-1}(f) + \alpha_3 \lambda_C(f) + \alpha_4 \lambda_{C^{-1}}(f), \quad (2)$$

with

$$\lambda_O(f) = \{\text{amount that } f \text{ is not onto}\},$$

$$\lambda_{1-1}(f) = \{\text{amount that } f \text{ is not } 1-1\},$$

$$\lambda_C(f) = \{\text{amount that } f \text{ is not continuous}\},$$

$$\lambda_{C^{-1}}(f) = \{\text{amount that } f^{-1} \text{ is not continuous}\}.$$

where we acknowledge that f^{-1} may not be well-defined. Furthermore, we require that weights $0 \leqslant \alpha_i$ satisfy $\Sigma \alpha_i = 1$. These measure based quantities can be computationally expensive. Therefore when performing parameter fitting (to find the "best" model), which requires multiple evaluations of the defect (cost) function, we often can find useful "surrogates" for these defect measures, with this term reflecting the broad approach from optimization theory to efficiently tackle problems with expensive cost functions.

Judgement of model quality must be in terms of how we choose to weight errors in each of the two phase spaces. Therefore we assume measure spaces $(D_1, \mathcal{A}_1, \mu_1)$ and $(D_2, \mathcal{A}_2, \mu_2)$, where $D_1 \subset X$ and $D_2 \subset Y$, $\mathcal{A}_1$ and $\mathcal{A}_2$ are σ-algebras, and μ_1 and μ_2 are measures. For technical correctness, we further assume the relative measures,

$$\overline{\mu_2}(f[A]) = \mu_2(f[A \cap D_1] \cap D_2), \quad (3)$$

for arbitrary set $A \subset X$. The idea is that we want to restrict ourselves to measuring image points that lie in D_2 whose preimage was in D_1. Similarly, we define

$$\overline{\mu_1}(f^{-1}[B]) = \mu_1(f^{-1}[B \cap D_2] \cap D_1). \quad (4)$$

D_1 and D_2 are "chosen" by the modeler as the portions of phase space which are of interest, and measures μ_1 and μ_2 allow the modeler to vary the relative importance of different parts of those sets. We refer to [15] for detailed definitions of $\lambda_O(f)$, $\lambda_{1-1}(f)$, $\lambda_C(f)$, and $\lambda_{C^{-1}}(f)$, which we summarize here.

To measure the onto deficiency, we desire to measure the fraction of D_2 which is not covered by the range of f. We define the *onto deficiency* λ_O of the function f by

$$\lambda_O(f) = 1 - \frac{\overline{\mu_2}(f[D_1])}{\mu_2(D_2)}. \quad (5)$$

Note that commonly, the commuter f may have fractal structure with the range of f a Cantor set. Therefore a simplifying "suitable surrogate," appropriate when D_2 is an in-

terval and μ_2 is absolutely continuous, is to quantify the lack of onto-ness by finding the "biggest hole" in the range of f,

$$G := D_2 - f[D_1], \tag{6}$$

then a suitable surrogate is given by

$$\tilde{\lambda}_O(f) := \sup_{I \subset G} m(I), \tag{7}$$

where I is an interval and m is Lebesgue measure.

To measure the $1-1$ *deficiency* of the commuter f, on the domain of f, we consider the extent of the "folding" [21], a measurement on the range, as well as measuring how much of the domain participates in that folding. We proceed as follows: we define $\mathcal{G}$ to be the collection of all subsets $G \subset D_1$ which satisfy that G is μ_1 measurable, $f[G]$ is μ_2 measurable, and f restricted to G is $1-1$. For any such G, we denote the complement in D_1 by $\bar{G} \equiv D_1 - G$. Then we define the $1-1$ *defect* by

$$\lambda_{1-1}(f) := \inf_{G \subset \mathcal{G}} \left[\frac{\mu_1(\bar{G})}{2\mu_1(D_1)} + \frac{\overline{\mu_2}(f[\bar{G}])}{2\mu_2(D_2)} \right]. \tag{8}$$

We may define a suitable surrogate in the standard case as follows. We may simply identify the largest part of the range that is multiply covered. We define envelope functions

$$e^+(x) = \sup_{D_1 \ni y \leqslant x} f(y), \quad e^-(x) = \inf_{D_1 \ni y \geqslant x} f(y). \tag{9}$$

Then $e^+(x)$ records the largest function value to the left of x, while $e^-(x)$ records the smallest function value to the right of x. Then

$$\tilde{\lambda}_{1-1}(f) = \| e^+(x) - e^-(x) \|_p \tag{10}$$

in terms of any p-norm, and we typically choose $p=\infty$.

To measure a *continuity deficiency*, we will take a measure-theoretic stance on the usual concept that continuous functions map "small sets to small sets." In particular, we seek to identify when the f undergoes a "jump," and measure the jump. However, to allow the possibility of Cantor sets for D_1 and D_2, we define in terms of measures of those sets. For each $x_0 \in D_1$ and for each $\delta > 0$, we define the set

$$\mathcal{B}(\delta, x_0) := \{x : x \in D_1, |x - x_0| < \delta\}, \tag{11}$$

which creates a nested family of sets as $\delta \searrow 0$. We measure the f-image of these sets by defining

$$a_\delta(x_0) := \inf_{I \supset f[\mathcal{B}(\delta, x_0)]} \frac{\mu_2(I \cap D_2)}{\mu_2(D_2)}. \tag{12}$$

Because $a_\delta(x_0)$ is monotonically decreasing with decreasing δ, we can take the limit as $\delta \searrow 0$, defining

$$a(x_0) := \lim_{\delta \to 0^+} a_\delta(x_0), \tag{13}$$

where we think of $a(x_0)$ as being the *atomic* part of f [16]. We define

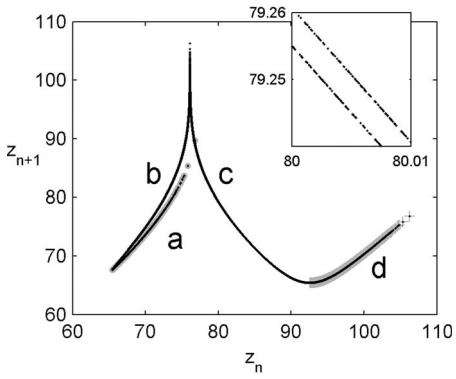

FIG. 3. Lorenz system, $\beta=8/3$, $\rho=60$, and $\sigma=10$. 500 000 iterates of the successive maxima map, with symbols assigned to regions of phase space. Observation of a trajectory reveals that the iterates associated with symbol d are always followed by symbol a. The inset highlights that although the map looks like a single curve at macroscopic scales, fine resolution reveals that the "curve" is actually a very thin fractal.

$$\lambda_C(f) := \sup_{x_0 \in D_1} a(x_0). \tag{14}$$

Note that if D_1 is an interval, we can define a suitable surrogate,

$$\tilde{\lambda}_C(f) = \| a(x_0) \|_p. \tag{15}$$

We note that $\tilde{\lambda}_C(f) \equiv \lambda_C(f)$ when $p=\infty$, but the flexibility to use other norms might prove useful in some situations.

V. APPLICATION—MODELING A LORENZ SYSTEM

As a concrete example of how *defect* can be used to find optimal models, consider the flow generated by the Lorenz system with parameters $\beta=8/3$, $\rho=60$, and $\sigma=10$. Although this system is quite different from that studied by [19], we still apply that crucial technique by considering the map of successive maxima. Figure 3 (panel 1) shows the plot of z_{n+1} vs z_n for a long trajectory on the attractor. Because of the strong contraction in the system, the resultant object "appears" to be one-dimensional when viewed from the macroscopic scale. With this motivating observation, we presume the following modeling goal: Find a one-dimensional (1D) map g_2 from the class of functions of constant magnitude slope that best models the dynamic behavior indicated by the successive maxima map, g_1. (Note: g_1 has no algebraic description. Rather, it reflects a long orbit along the attractor known only as a finite sequence of data, $\{z_i\}$, the sequence of successive maxima. Therefore it serves to illustrate how this technique can be applied in modeling a physical system from time series.)

A key step in developing commuters is to assign a partition in each of the spaces, where partitioning can be viewed as equivalent to the symbol dynamics operation of assigning a symbol to each region of phase space [4]. For 1D maps, a typical partition assigns a symbol to each monotone segment. If we ignore the fine scale structure, the maxima map admits a very natural four-symbol partition, as illustrated by Fig. 3.

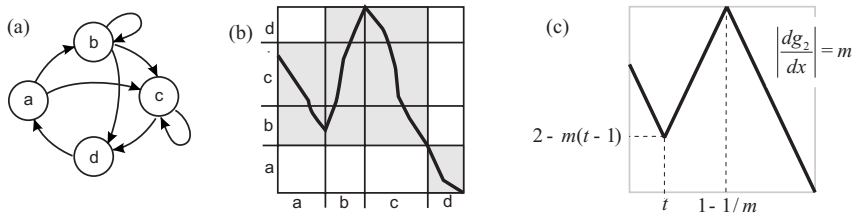

FIG. 4. (a) A transition graph shows the symbol dynamics observed in the trajectory, with symbol assignment as in Fig. 3. (b) We capture the same symbol dynamics by a 1D continuous map of the interval. The grayed blocks indicate the allowed symbol transitions, and the curve drawn through the gray blocks is a possible choice of 1D map that yields those symbol transitions. Note that we are not requiring a Markov property of the partition, so that the map need not map exactly across a partition [4]. (c) From our assumed modeling class (maps of constant magnitude slope), we show a (typical) member of subset of that class which is consistent with the required symbol dynamics. The family of such maps are parametrized over the slope magnitude, m, and the turning point, t.

Observation of a trajectory of the maxima map reveals that points assigned to symbol d always iterate to points assigned to symbol a. By requiring that our model have the same allowable symbol transitions as g_1, we are led to consider candidate models of the form in Fig. 4, where a member of the family of models is determined by parameters m and t, and we denote the resultant map as $g_{2(m,t)}$. This map is the linear interpolation with nodes at the points

$$(0,2-m+2mt), \quad (t,2-m+mt), \quad (1-1/m,1), \quad (1,0).$$

When there is no confusion, or when we are addressing the general case, we will simplify notation and denote $g_{2(m,t)}$ simply as g_2. We note that

$$|g_2'| = m \tag{16}$$

except at the knots.

Developing a "good" model equates to choosing parameter values m and t that create model dynamics that are similar to the dynamics of g_1. No standard technique exists for making this choice. Note that Eq. (17) gives the expansion rate everywhere on the interval, and it immediately follows that both metric and topological entropy of any $g_{2(m,t)}$ is $\ln m$ [6]. Consequently parameter estimation using entropy methods will be unable to provide means to select t. Rather, we get the best dynamical match by choosing m and t so that the resultant commuter is as close as possible to being a conjugacy. For a fixed choice of parameter values, we solve the functional equation

$$g_{2(m,n)} \circ f_{m,t} = f_{m,t} \circ g_1, \tag{17}$$

to find the commuter $f_{m,t}$, computed as the fixed point of the operator

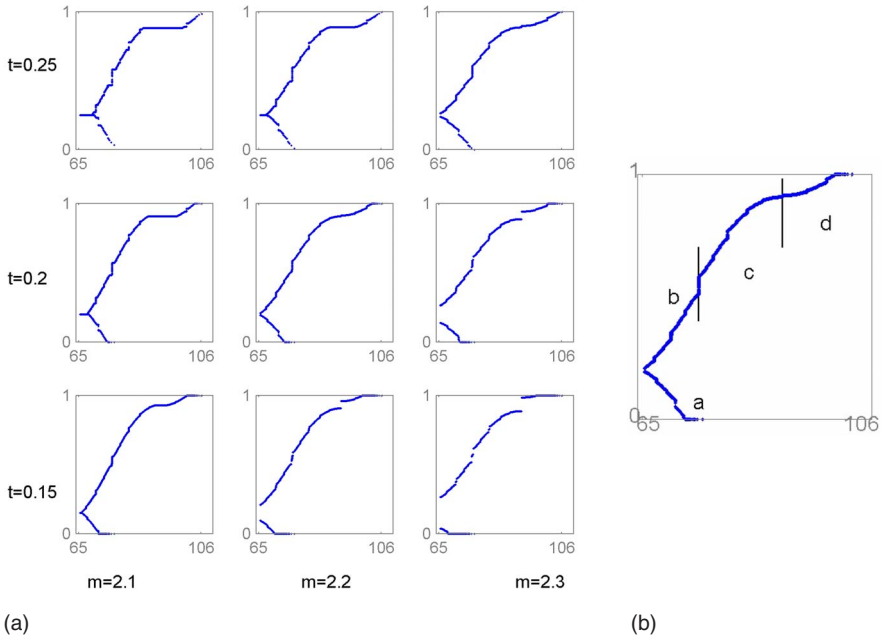

FIG. 5. (Color online) Commuter functions. (a) Commuter functions $f_{m,t}$ between the Lorenz system and models $g_{2(m,t)}$ for several choices of parameter values. For ease of visualization, we choose to provide a branched description of the commuter, where the lower branch may be associated with symbol a. (b) The $m=2.2$, $t=0.2$ commuter is label with the symbol that is associated with each region of the domain space.

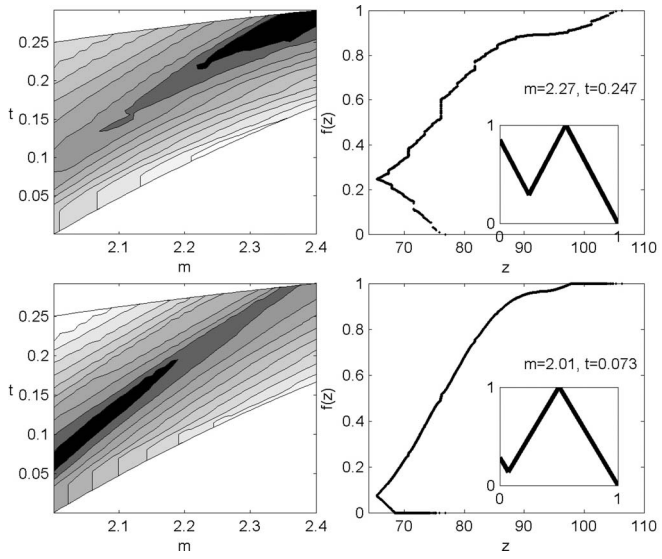

FIG. 6. Contour plot of "defect" over parameter space (a,c) and associated commuter (b,d) for the optimal model (inset). The top row (a,b) computes defect using the Lesbegue measure on the horizontal, while the bottom row (c,d) of plots is based on the natural measure on the horizontal.

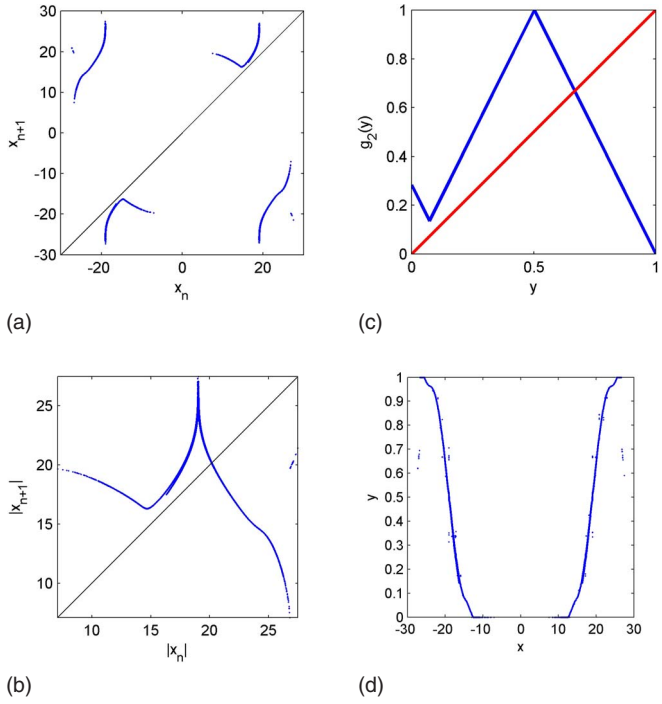

FIG. 7. (Color online) Comparing Poincaré map to the model. (a) The successive return map has disjoint components but appears nearly one-dimensional. (b) By taking absolute values, we see the symmetry projection is shaped similar to our model of the successive maxima. (c) The optimal model from the successive maxima, $g_{2(2.01,0.73)}$, is used as a comparative map; and (d) the resultant commuter between $g_3(x)$ and $g_2(y)$, the linear model. The "fuzziness" in the commuter is expected, since the map g_3 lies on a fractal object which is higher than one-dimensional.

$$C(f) = g_{2(m,n)}^{-1} \circ f \circ g_1. \tag{18}$$

Because g_1 is known only at each z_i, the commuter f is approximated by computing only at these same ordinates, so that $g_1(z_i) =: z_{i+1}$ contributes no error to the computation of $g_2^{-1} \circ f \circ g_1$. Figure 5 shows examples to *visually* assess which might be the best commuter, since homeomorphism would be optimal.

To find the "best" model, we use *defect* as a cost function to "measure" the difference between the Lorenz system and a model. Because $f_{m,t}$ is computed on a finite set of ordinates, measure based computations can be problematic. To simplify, we use surrogate methods to compute a defect. Let

$$\begin{aligned}\tilde{\lambda}(f) = &[\text{largest vertical gap in each branch}] \\ &+ [\text{vertical gap between branches}] \\ &+ [\text{largest horizontal segment in each branch}].\end{aligned}$$

This choice of defect ignores fine scale many-to-oneness of the commuter. These small scale variations are consequences of the fact that the maxima map is not a curve, but a thin, fractal structure. Ignoring the fine scale "fuzziness" of the commuter is consistent with our modeling goal of simplification.

If we use the Lebesgue measure of intervals, then evaluation of the defect on a grid of parameter values indicates that a good choice for the parameters is $m=2.27$, $t=0.247$. As an alternative approach, the modeler might decide that it is more important for the model to accurately capture the dynamics which are most frequently observed. Then instead of the Lebesgue measure on D_1, one would choose the natural measure on the dynamics, which we assume is reflected by the density of points in the long trajectory. To account for this change of emphasis, we measure horizontal segments not by their geometric length but by the fraction of the z_i that falls in that interval. Recomputing the defect over the grid of parameter values, we find that the modeler should choose $m \approx 2.01$, $t \approx 0.073$. We emphasize that the expert knowledge of the modeler remains a crucial input to this process as the modeler must decide what is "important" for the model to be able to describe. The techniques simply give the modeler a principled way to select the parameter values. Figure 6 illustrates this method of parameter selection.

Despite the continued popularity and historical significance [1], it is known that the z-successive maxima map is not an embedding because successive maxima of $z(t)$ are simply the zero-crossings Poincaré section on the derivative of z, on which there is a symmetry. In other words, the observation function is given by $\alpha(x,y,z)=(z) \coloneqq xy-bz$. The symmetry of this observer in the x,y variables means that there is no way to distinguish x from y using this observation. Hence the measurement function is "nongeneric" in the language of the family of Taken's embedding type theorems, in that there is no conjugacy between the delay embedding and proper Poincaré map. We remark that conjugate modeling is not the thesis of our paper—our formalism is meant to allow comparison between dynamics which are not necessarily conjugate. Real data sets cannot always be guaranteed to

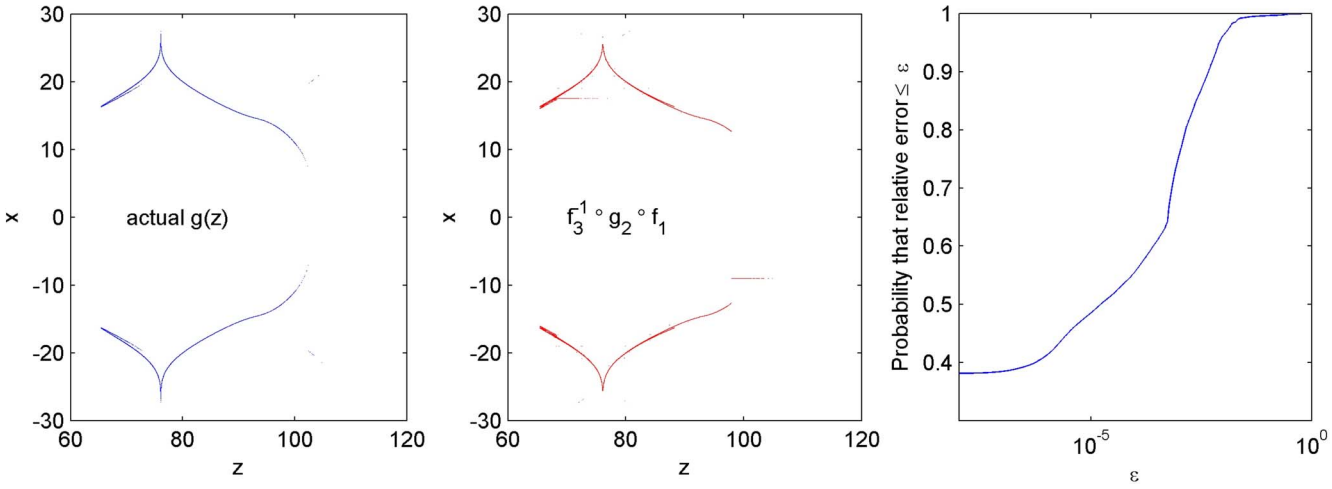

FIG. 8. (Color online) Analyzing model fidelity. (a) The exact relationship $x=g(z)$ as found by integration using a long trajectory to create 100 000 (z,x) pairs. (b) Using the same ordinates as the left panel, we use nearest-neighbor interpolation to find $f_3^{-1}\circ g_2\circ f_1$. (c) The relative error of the approximation is computed for each of the 100 000 points, and collected statistics are organized in a cumulative distribution plot showing the fraction of the data points whose error is less than ϵ. We note that about 40% of the points are accurate to machine precision, while >90% have relative error smaller than 0.005. Large errors represents the information loss by forcing the intermediate representation of g_2, where we know that information must be lost because g_2 is not conjugate.

be embeddings, and we have presented a method to best model such data sets without the restriction of requiring conjugacy. However, in this case we do have the Lorenz equations of motion for which one can construct a true Poincaré section, and we may use this as a means to test the robustness of the approach.

To continue with our data driven approach, we assume that the x and z components of the Lorenz system are a measurable variable in some unknown continuous process. We construct a sequence $\{x_i\}$ of crossings of the plane $z=64$. This plane is selected based on the observed time series, to retain the "realism" of the process as having come from a physical system (as opposed to selecting the plane using analytic methods, such as described in [22]). For the given sequence, we can define

$$g_3(x_i) := x_{i+1}$$

as the successive maxima map. By exploiting the symmetry in the return map, we compare the dynamical properties of the return map to the *optimal model of the successive maxima.* The resultant commuter is a 2-1 projection, as should be expected. The Poincaré map analysis data is shown in Fig. 7.

If we denote the commuter from g_1 to g_2 as f_1 and denote the commuter from g_3 to g_2 by f_3, then we can envision the relationships by the commutative diagram:

$$\begin{array}{ccc} Z & \xrightarrow{g_1} & Z \\ f_1\downarrow & & \downarrow f_1 \\ Y & \xrightarrow{g_2} & Y \\ f_3\uparrow & & \uparrow f_3 \\ X & \xrightarrow{g_3} & X \end{array} . \tag{19}$$

We note that when we project the "real" dynamics to the model, we are projecting onto one-dimensional dynamics, so we expect that information (fine scale orbit structure) will be lost. Additionally, just as a linear regression is not a perfect model, that projection has error—additional dynamics which are not present in the original system. To assess the validity of our overall approach we note that from a particular Poincaré section crossing x_j, we may integrate to the next maxima in z, and from there, integrate further, to the next crossing at x_{j+1}. Then along a particular trajectory on the attractor, each maxima (recorded as a z value) is followed deterministically by an x value at the subsequent crossing. By abuse of notation, we can envision a relationship

$$x = g(z)$$

that describes a set of points in the z-x plane which will appear to be nearly a one-dimensional curve (but slightly thicker). Obviously, the symmetry created causes us to expect two x values for each z. Because Eq. (19) does not describe conjugacy relationships, the best that we can expect is that

$$g(z) \approx f_3^{-1} \circ g_2 \circ f_1. \tag{20}$$

We note that on the right-hand side of Eq. (20), we are expecting our linear model g_2 to describe the dynamics. Comparison of $g(z)$ with $f_3^{-1}\circ g_2\circ f_1$ in Fig. 8 indicates the fidelity of model g_2.

VI. CONCLUSION

Here, we have opened a discussion of how the art of modeling can be cast in the language of dynamical systems by an appropriate extension of the usual notion of conjugacy

to the generalized concept to measure a defect in a commuter function. We have discussed parameter estimation within this context, leading to a well-defined concept of quality of simplified toy models representing the nature of the dynamics of a full system. We have noted that expert knowledge of the modeler need not, and even should not, be mathematically removed from the process.

ACKNOWLEDGMENTS

This work was supported by the NSF under Grant No. DMS-0708083. We would also like to thank the referee for very useful comments which significantly improved the revised version of this paper.

[1] E. Lorenz, Tellus **17**, 321 (1965).
[2] E. N. Lorenz and K. A. Emanuel, J. Atmos. Sci. **55**, 399 (1998).
[3] H. Poincare, *Les M'ethods Nouvelles de la M'ecanique C'eleste* (Gauthier-Villars, Paris, 1892).
[4] C. Robinson, *Dynamical Systems; Stability, Symbolic Dynamics, and Chaos*, 2nd ed. (CRC Press, Boca Raton, FL, 1999).
[5] B. Kitchens, *Symbolic Dynamics, One-sided, Two-sided and Countable State Markov Shifts* (Springer, New York, 1998).
[6] E. Ott, *Chaos in Dynamical Systems*, 2nd ed. (Cambridge University Press, Cambridge, England 2002).
[7] J. Guckenheimer and P. Holmes, *Nonlinear oscillations, dynamical systems, and bifurcations of vector fields* (Springer, New York, 1982).
[8] R. L. Devaney, *An Introduction to Chaotic Dynamical Systems*, 2nd ed. (Westview, New York, 2003).
[9] C. H. Reinsch, Numer. Math. **10**, 177 (1967).
[10] C. H. Reinsch, Numer. Math. **16**, 451 (1971).
[11] *Matlab, Spline Toolbox, CSAPS* 7th ed. (Mathworks, Natick, MA, 2006).
[12] E. M. Bollt and M. Dolnik, Phys. Rev. E **55**, 6404 (1997).
[13] M. Dolnik and E. M. Bollt, Chaos **8**, 702 (1998).
[14] D. Lind and B. Marcus, *An Introduction to Symbolic Dynamics and Coding* (Cambridge Univversity Press, New York, 1995).
[15] J. D. Skufca and E. M. Bollt (unpublished).
[16] By *atomic part*, we mean to use the Lebesgue decomposition of a function [17] into its continuous part and atomic part, $f(x)=c(x)+a(x)$. The theorem applies to functions of bounded variation, and sometimes f will not satisfy this hypothesis. However, since we do not require an actual decomposition, we view our verbiage as a minor abuse of notation. See [18] for a further discussion of this general decomposition.
[17] A. Kolmogorov and S. Fomin, *Introductory Real Analysis* (Dover, New York, 1975).
[18] P. Halmos, *Measure Theory* (Springer, New York, 1974).
[19] E. N. Lorenz, J. Atmos. Sci. **20**, 130 (1963).
[20] A smoothing spline is a minimization of the functional, $\mu\Sigma_{i=1}^{n}|y_i-f(x_i)|^2+(1-\mu)\int|D^2f(t)|^2dt$, within the class of piecewise polynomial functions. The convex combination balances the competing elements of the usual least-squares approximation when $\mu=0$ and a spline interpolant through all the points when $\mu=1$ [9–11].
[21] By "folding," we mean to measure many-to-oneness, quantifying the amount of the range which has multiple preimages.
[22] C. Sparrow, *The Lorenz Equations: Bifurcations, Chaos and Strange Attractors* (Applied Mathematical Sciences, Springer, New York, 1982).